



## Improving the Use of Mixing Factors for Dilution Ventilation Design

Charles E. Feigley , James S. Bennett , E. Lee & Jamil Khan

To cite this article: Charles E. Feigley , James S. Bennett , E. Lee & Jamil Khan (2002) Improving the Use of Mixing Factors for Dilution Ventilation Design, Applied Occupational and Environmental Hygiene, 17:5, 333-343, DOI: [10.1080/10473220252864932](https://doi.org/10.1080/10473220252864932)

To link to this article: <https://doi.org/10.1080/10473220252864932>



Published online: 30 Nov 2010.



Submit your article to this journal [↗](#)



Article views: 130



View related articles [↗](#)



Citing articles: 7 View citing articles [↗](#)

# Improving the Use of Mixing Factors for Dilution Ventilation Design

Charles E. Feigley,<sup>1</sup> James S. Bennett,<sup>1</sup> E. Lee,<sup>1</sup> and Jamil Khan<sup>2</sup>

<sup>1</sup>Department of Environmental Health Sciences, School of Public Health, University of South Carolina, Columbia, South Carolina; <sup>2</sup>Department of Mechanical Engineering, University of South Carolina, Columbia, South Carolina

---

In specifying dilution ventilation flow rate, a safety factor,  $K$ , is often used to provide a margin of safety and to compensate for uncertainties and health impact severity. In current practice, the selection of  $K$  is very subjective. Here the component of  $K$  accounting for imperfect mixing,  $K_m$ , was studied to develop more effective and efficient design procedures. Air flow and contaminant distribution in a 10 m × 3 m × 7 m room with a single contaminant source on a 1-m high table were simulated for steady, isothermal conditions using computational fluid dynamics. A series of 10 simulations explored factorial combinations of air exchange rates (1, 2, 4, 8, 16 ACH) and inlet types (a high wall jet and a ceiling diffuser). Nine additional simulations explored exhaust opening location effects and 13 other simulations investigated source location effects.  $K_m$  was calculated at each of 25,600 grid locations within the room by linear regression of emission rate/flow rate ( $G/Q$ ) on concentration ( $C$ ). The linear relationship between  $C$  and  $G/Q$  at each of the points was nearly perfect ( $R^2 \geq 0.97$ ). For the simulations with varying dilution flow rate,  $K_m$  ranged from 0.19 to 2.86 for the wall jet and from 0.94 to 4.34 for the ceiling diffuser. Holding  $G/Q$  at 100 ppm and varying source and exhaust location produced room average concentrations from 55.7 to 173 ppm. Unlike orthodox design approaches, this work suggests that air monitoring data often can be used to calculate dilution flow rate requirements. Also, dilution flow rate requirements may be reduced by enhancing room mixing with fans or altering air inlet configuration. However, mixing should not be increased if the altered room air currents could transport contaminant to an occupant's breathing zone or interfere with other control methods that depend on segregation of incoming air and contaminant.

---

**Keywords** Dilution, Safety Factor, Mixing Factor, Computational Fluid Dynamics, Indoor Air, Industrial Hygiene Engineering, Industrial Ventilation

An equation for calculating dilution air flow rate requirements for controlling exposure to airborne contaminants in a room often is derived by assuming that the room is well mixed.<sup>(1)</sup> Solving the contaminant mass balance for steady-state conditions and clean dilution air, and adding a safety factor yields the familiar equation:<sup>(1)</sup>

$$Q = K \frac{G}{C} \quad [1]$$

where

- $Q$  = dilution air flow rate,
- $C$  = target contaminant concentration, such as an occupational exposure limit,
- $G$  = contaminant emission rate, and
- $K$  = multipurpose safety factor.

The safety factor is used to account for a variety of uncertainties and concerns, including deviations from the assumption of complete mixing, the severity of contaminant health effects, and the number of workers exposed.

In rooms with an active contaminant source and clean dilution air flow, very high contaminant concentrations are found immediately downwind of the source (also in the wake persons standing upwind of the source) and very low concentrations are found in the inlet air stream. Thus, such rooms are not well mixed, at least in a strict sense. In 1946, Lidwell and Lovelock<sup>(2)</sup> recommended the use of a “mixing factor” to compensate for the assumption of complete mixing. This mixing factor was the effective air exchange rate for dilution of a contaminant at a specific point within the room.

Later, Brief<sup>(3)</sup> extended the concept of the mixing factor to account for contaminant toxicity considerations and the locations of air inlets, air outlets, and contaminant sources. This adjustment, essentially the inverse of that used in Eq. 1, is more accurately termed a “safety” factor because it accounts for other effects in addition to nonuniform contaminant mixing. More recently, Burton<sup>(4)</sup> noted that mixing factors generally range from 1.0 to 3, and suggests that improved mixing, or control measures other than dilution ventilation, be considered if the appropriate

values exceed 2. Also, the use of a mixing factor for assessing exposures was suggested by Jayjock.<sup>(5)</sup>

In recent versions of its standard for achieving acceptable indoor air quality, the American Society for Heating, Refrigerating and Air Conditioning Engineers (ASHRAE) accounts for incomplete mixing in indoor spaces.<sup>(6)</sup> The “ventilation effectiveness” ( $E_v$ ), as used by ASHRAE, is the fraction of outdoor dilution air entering a room that reaches the occupied zone.  $E_v$  is similar to the mixing factor used in industrial applications except that it applies to the occupied zone rather than an entire room.

Heinsohn<sup>(7)</sup> discussed several measures of mixing and recognized that measures such as the effectiveness coefficient and the “age of air” vary with location within a room. Although useful for understanding air flow and contaminant transport, these concepts are seldom applied in ventilation design. Indeed the simple approach using Eq. 1 appears to be the most commonly employed method for steady-state conditions.

The specification of dilution ventilation safety factors has been recognized to be “a very uncertain art, not a science” and treating mixing and toxicity separately has been suggested.<sup>(8)</sup> Also, the use of a single value of  $K$  to describe the effective ventilation for an entire room has been opposed on grounds that it violates the contaminant mass balance.<sup>(9)</sup> Heinsohn<sup>(7)</sup> pointed out flaws in the conventional use of mixing factors, including: (1) a scalar multiplier is not justified by scientific principles; (2) experimentally determined mixing factors are unique to flow rate, geometry, locations of air handling duct openings, and the measurement point; (3) the value of the mixing factor cannot be predicted with any precision; and (4) the range of mixing factors is too large for effective design and economic analysis. Nevertheless, the use of safety factors, selected by professional judgment, has become a standard procedure for specifying dilution air flow requirements.<sup>(1)</sup>

Clearly, better ways of dealing with nonuniform concentrations in rooms must be developed to ensure efficient and effective worker protection. Here the goal is to generate hypotheses for improving dilution ventilation design, particularly the treatment of spatial variation within a room. In this study,  $K$  is considered to be the product of separate factors for specific sources of uncertainty, as suggested by others (e.g., ASHRAE Standard 62-1999<sup>(6)</sup>):

$$K = K_m \cdot K_t \cdot \dots \cdot K_n \quad [2]$$

where

$K_m$  = mixing factor,

$K_t$  = toxic effect severity factor,

$K_n$  =  $n^{\text{th}}$  component factor.

Only the component of  $K$  dealing with mixing,  $K_m$ , is considered here. The specific objectives were: (1) to see how increasing dilution air flow rate affects the contaminant concentration throughout a room, and thus the selection of  $K_m$ ; and (2) to explore the effects of various contaminant source, air inlet, and air outlet locations on  $K_m$ .

## METHODS

Focusing on mixing and ignoring other components of the safety factor,  $K_m$  equals  $QC/G$  from Eq. 1. Because  $C$  varies within an incompletely mixed room, separate values of  $K_m$  may be calculated at each point within a room. The final design value of  $K_m$  may then be selected to provide control at a specific room location or throughout some portion of the room. Thus, determination of  $K_m$  for a room requires the ability to estimate concentration throughout a room. There are two basic approaches for accomplishing this: monitoring contaminant concentration in a space with controlled air flow, or using mathematical methods to estimate the concentration throughout a space. Numerical solution of the fundamental equations governing fluid flow and contaminant transport, called computational fluid dynamics (CFD), was used here because CFD allowed rapid exploration of the effects of a variety of room configurations, flow rates, and emission rates, and provided finely resolved concentration estimates throughout the rooms.<sup>(10)</sup> (Terms related to CFD used here appear in the glossary at the end of this article.)

Accurate CFD simulation of a particular room requires careful characterization of inlet flow patterns, sources, and thermal boundary conditions. It also relies on assumptions including the treatment of turbulence and near-wall fluid phenomena. Thus, accurate simulation of contaminant distribution in a real room using CFD requires validation. Here we used CFD to obtain insight into the behavior of hypothetical rooms, not to predict the behavior of any specific room. Nevertheless, several types of validations were undertaken, including comparison with observations from full size rooms under controlled conditions and comparison with observations from a scale model of the room simulated here.

CFD accuracy for predicting concentration or velocity is touched on in many studies, but few deal with accuracy in detail. Reviewing CFD applications in indoor environments, Emmerich<sup>(11)</sup> found eight studies reporting good quantitative agreement with measurements, four reporting good qualitative agreement but poor quantitative agreement, and four reporting problems with CFD prediction accuracy. Of the latter category, one attributed inaccuracies to poorly known boundary conditions. Others in this category were attempts to deal with predominantly natural convection or mixed convection, and/or predict air exchange among multiple compartments. Overall, it appears that CFD has been used successfully to simulate flow in single compartments, even in spaces with combined radiative and convective heat transfer, but poorly characterized boundary conditions can result in large differences between CFD results and observation.

## Validations of CFD Simulation Approaches

To ensure that the CFD approaches used here were able to produce plausible concentration distributions, several types of validation studies were performed. The solution methods were validated for grid independence, physical plausibility, and ability to simulate experimental data. Validation is summarized

here, but has been presented in detail elsewhere.<sup>(12)</sup> The results from a  $30 \times 24 \times 36$  grid were compared with results from a  $60 \times 24 \times 36$  grid. As a measure of physical plausibility under steady-state conditions, the average exhaust concentration was compared to  $G/Q$ . To externally validate the simulations, measured velocities from a full-sized room reported in the literature<sup>(13)</sup> were compared with numerical simulations of that room using CFD methods identical to those used for the hypothetical rooms considered here.

In addition to the validation approaches above, a scale model was constructed, experimentally characterized, and simulated with CFD. Based on geometric and kinematic similarity criteria,<sup>(14)</sup> a scale model of a room similar to the one used in the CFD runs was constructed. The model is 1 m long by 0.7 m wide by 0.3 m high and made of 0.5-inch Lexan. Sampling ports were drilled in the top of the chamber to allow insertion of a sampling probe. Pure isobutylene was used as a tracer gas and measured with a photoionization (PI) analyzer (Model 101, HNu Systems, Inc., now Process Analyzers, LLC, Walpole, MA). At constant isobutylene and dilution air flow rates, chamber air was sampled at three heights from the floor: bottom (3.7 cm), middle (13.7 cm), and top (23.7 cm). Concentration was measured at a total of 117 points: 104 sampling points at the center of the cells with the dimension of 0.2 m(L)  $\times$  0.1 m(H)  $\times$  0.1 m(W), plus 12 extra sampling points near the source and 1 in the outlet gas stream. Three complete sets of measurements were collected on different days. A StowAway<sup>®</sup> Voltage Logger (Onset Computer Corp., Onset, MA) was used to collect concentration data for a 20-second period at each point. Three replicate runs were performed. Then the chamber was simulated using CFD approaches identical to those used to simulate the hypothetical rooms described below. Simulation inlet velocities were based on the measured velocities at the chamber air inlet.

### CFD Room Simulations

Ten simulations of air flow and contaminant dispersion in a hypothetical room were performed at factorial combinations of 2 dilution air inlets and 5 air flow rates. Next, 22 simulations were performed at a single flow rate for various locations of the contaminant source and the air outlet.

To ensure that conditions explored represent those that reasonably may be found in real rooms, a spreadsheet containing the design procedures for side-wall supply and ceiling supply ventilation given by Awbi<sup>(14)</sup> was developed and used to check the configuration of the room and ventilation parameters. The room length and height were arbitrarily chosen to be 10 m and 3 m, and the horizontal aspect ratio ( $W/L = 0.7$ ) was selected to provide some deviation from a square, yet stay within the range of aspect ratios recommended<sup>(14)</sup> for a single, centrally located ceiling diffuser.

The estimated average air speed in the room occupied zone (lowest 1.8 m for standing work) was kept close to recommended comfort limits.<sup>(15,16)</sup> Also, for the wall supply, the maximum inlet jet drop was kept reasonable and the supply was located

close enough to the ceiling to prevent separation of the jet from the ceiling. The air exchange rates selected for simulation are 1, 2, 4, 8, and 16 air changes per hour (ACH). The effects of two different dilution air inlets were explored: (1) a 1.4 m by 0.6 m rectangular high wall jet, and (2) a 0.6 m by 0.6 m, 3-vane, drop-in diffuser.

A standing work surface was represented by a 1-m cube at the center of the room with a 0.2-m square opening in the center of the cube's upper surface serving as the contaminant source. The 1-m surface height was chosen because it is nearly midway between two recommended heights for a standing workplace. A height of 107 cm is recommended for light assembly, writing, and packing tasks, and a height of 91 cm is recommended for tasks requiring large downward or sideward forces.<sup>(17)</sup>

The five air flow rates were investigated for each of two inlet diffuser locations. The contaminant emission rate was specified as  $2.33 \times 10^{-5}$  m<sup>3</sup>/s, an arbitrary rate that yields a  $G/Q$  value of 100 ppm at 4 air changes per hour (ACH). The following conditions were employed for all simulations: (1) gas phase contaminant, (2) steady-state, (3) negligible contaminant sinks, (4) no mechanical stirring, (5) negligible emission velocity, (6) air outlet not close to source (i.e., no intentional local exhaust), (7) isothermal conditions (no heat sources or air supply buoyancy), (8) no obstructions in the room except the work table, (9) clean dilution air, and (10) inlet velocity uniform and normal to the inlet face.

The numerical simulations were performed with commercial CFD software (structured Fluent, V. 4.2, Fluent Inc., Lebanon, NH), which uses the control volume method and the SIMPLE algorithm described by Patankar.<sup>(10)</sup> The  $k$ - $\epsilon$  turbulence model was chosen for economy, as it requires less computational effort than more sophisticated models. The room simulation used a uniform grid of 0.2-m cubic cells. The solution was considered converged if the sum of the normalized residuals was less than  $10^{-5}$ . The turbulence intensity was taken as ten percent, a common practice when this quantity is not measured. The characteristic length scales were set at 1.4 m, the width of the inlet (no grill present), for the wall jet, and at 0.038 m (1.5 inches), the distance between vanes of the diffuser, for the ceiling inlet because an eddy can be no larger than the largest flow boundary allows.<sup>(18)</sup>

Separately for the two inlets studied, the value of  $K_m$  was calculated at each of the 25,600 solution nodes within the room by regression with no intercept term. Each regression was based on 5 pairs of  $C$  and  $G/Q$  values from the 5 flow rates studied. These computations were performed within a Fortran 90 program using the IMSL regression subroutine, RONE. Further statistical analysis of  $K_m$  was performed using SAS (Statistical Analysis System, SAS Institute, Cary, NC).

## RESULTS

### Validations of CFD Simulation Approaches

The mean node-to-node difference between the concentrations from the  $30 \times 24 \times 36$  cell grid and the concentrations

from a grid with twice as many cells was only  $-0.3$  percent. Thus, to shorten the computation time, the coarser of the two grids was used. The mass balance of the contaminant in these two runs was checked by integrating the contaminant concentration across the outlet duct. The product of the average concentration and the flow rate was compared with  $G$ , the contaminant emission rate. Agreement was within 1 percent for both grids.

One external validation exercise was the comparison of CFD simulation results with experimental observations. The air speed and three-dimensional velocity components data measured at points in a three-dimensional grid throughout an experimental room were obtained from Dr. Mohammad Hosni at Kansas State University.<sup>(13)</sup> The air speed (i.e., the directionless magnitude of velocity) was used instead of velocity components, which were below the useable range of the instrument for large portions of the room. The difference between observed and simulated air speed was less than 30 percent in the occupied portions of the room, defined here as all the room below a height of 2 m. Also, the difference was negligible for a large portion of the breathing zone (BZ) plane. Although reasonably good agreement was

achieved, some concerns remained. First, the use of air speed instead of velocity was less than ideal. Second, some of the boundary conditions were not well characterized. For instance, inlet velocity distribution was not measured, forcing us to assume, in our simulation of this room, uniform inlet air velocity based on the measured flow rate.

The results of the second validation exercise, the comparison of CFD simulation of concentration distribution with experimental measurements for the scale model experiments, are shown Table I. The mean simulated concentrations at three elevations within the chamber are compared with the mean observed concentrations at these levels. Only the mean for the uppermost elevation was significantly different from the observed mean. The overall means and the means at the chamber middle and lowest levels were not significantly different.

Figure 1 compares the experimental isobutylene concentrations and the concentrations simulated using the observed inlet velocity profile. It is evident that the CFD-derived concentration distributions agreed well with the observed data. Overall, this validation exercise showed that the CFD approaches used here,

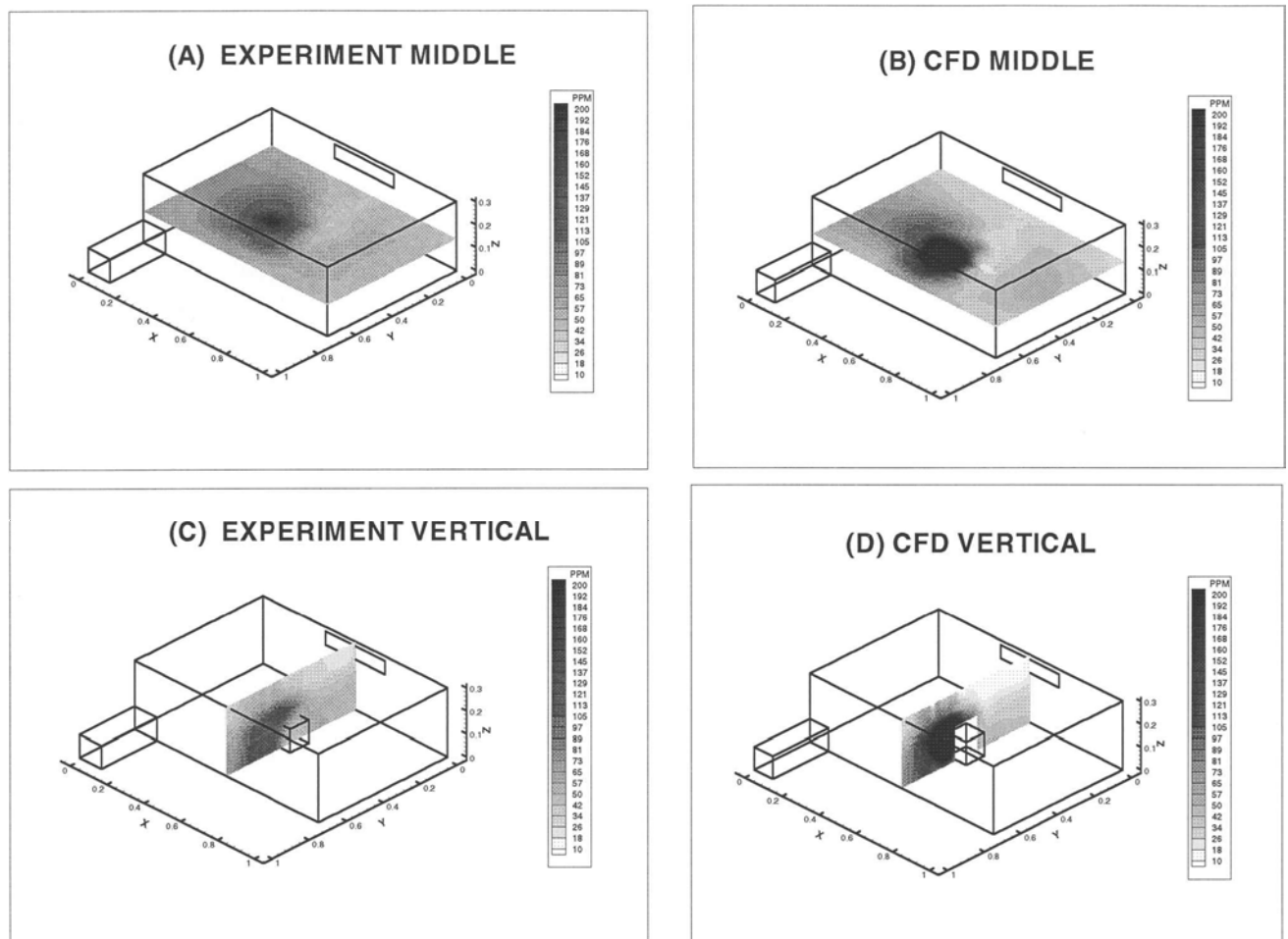


**FIGURE 1**

Comparison of experimental and CFD simulation concentration distributions.

**TABLE I**

Comparison of mean concentrations from two simulations with experimental mean concentrations

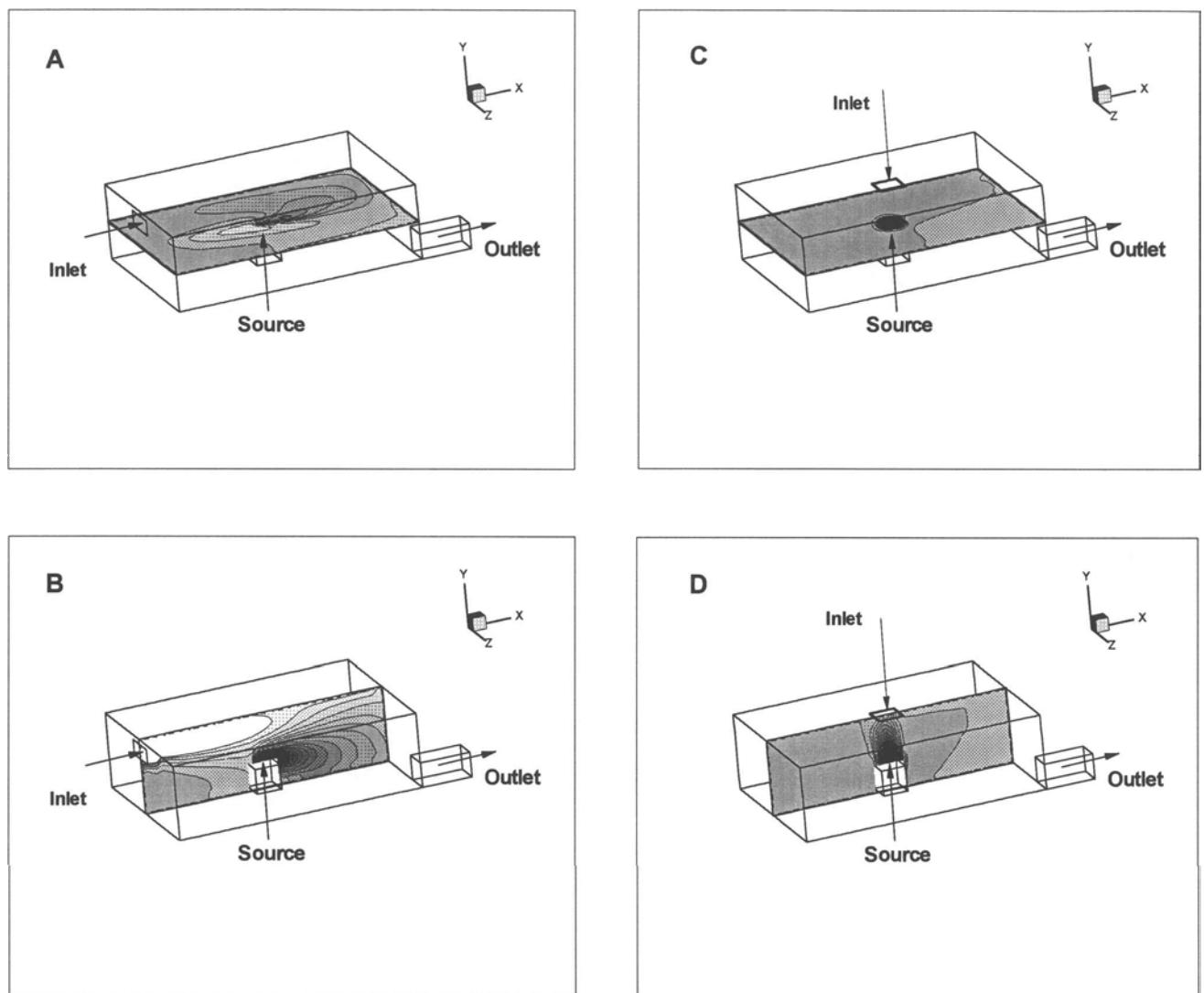
Level	N	Mean concentration (ppm)	
		Experimental	CFD
Bottom	38	76.9	76.8
Middle	39	77.0	84.1
Top	39	54.7	39.4 <sup>A</sup>
All	116	69.5	65.0

<sup>A</sup>CFD mean value significantly different from experimental mean values at the  $p \leq 0.05$  level.

including the grid characteristics and the treatment of turbulence and boundary conditions, performed well in modeling a chamber geometrically and kinematically similar to the simulated rooms. Thus, it appears that CFD is a valid means of generating plausible concentration distributions for these hypothetical rooms.

### Simulations of Hypothetical Rooms with Varying Flow Rates

For an air flow of 4 ACH and the wall jet inlet, Figures 2A and 2B show the simulated concentration contours in the breathing zone planes ( $Y = 1.5$  m) and in a vertical planes through the source ( $Z = 3.5$  m). The air velocity vectors for this air flow and inlet are shown in Figure 3A. The relative concentration patterns

**FIGURE 2**

Comparison of wall jet (A and B) and ceiling diffuser (C and D) simulated concentration distributions for a dilution air flow rate of four air changes per hour.

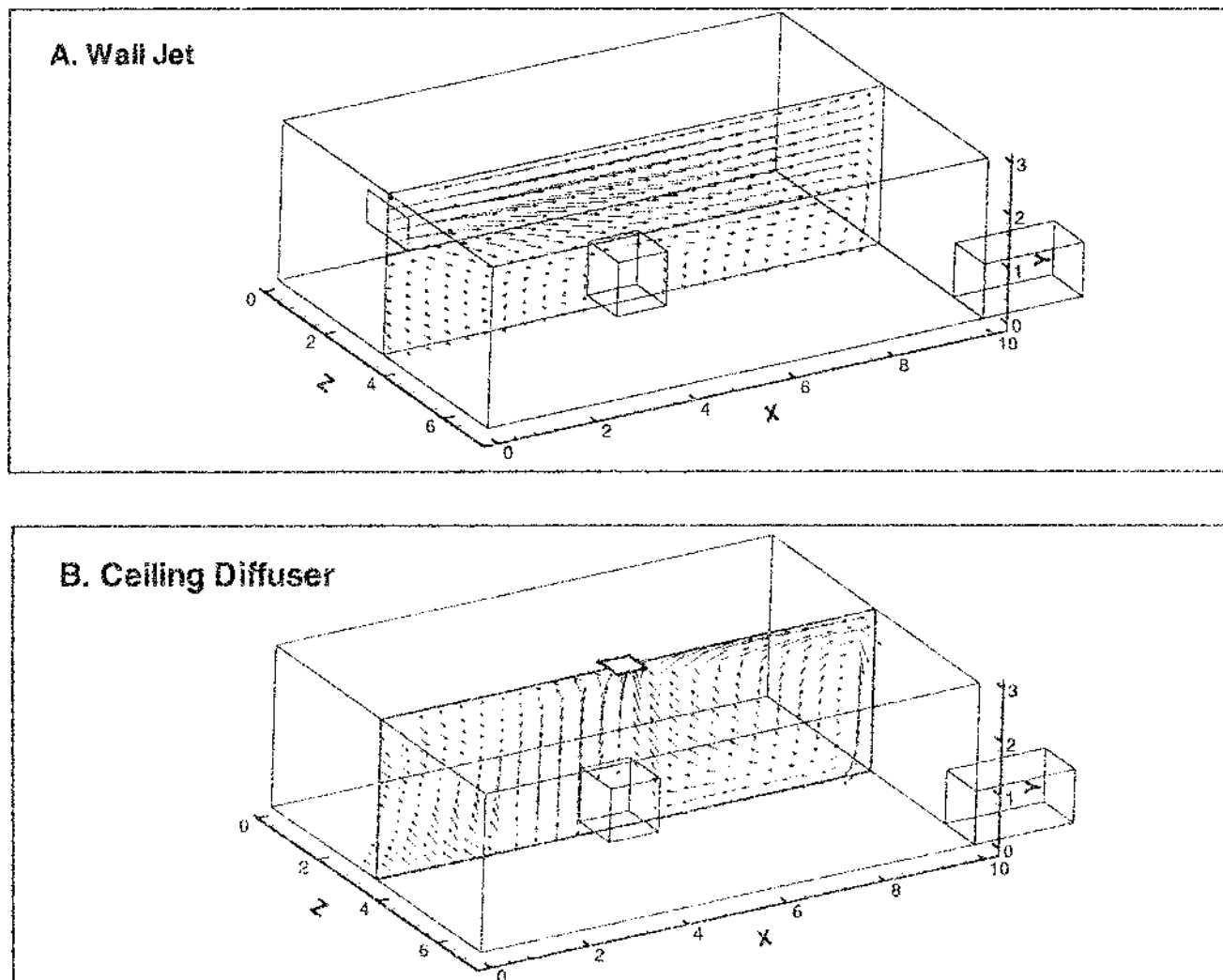


**FIGURE 3**

Comparison of simulated velocity vectors in a vertical plane for wall jet and ceiling diffuser inlets at a dilution air flow rate of four air changes per hour.

were essentially the same for all five flow rates. As the horizontal air jet flows along the ceiling, it expands downward, entraining air at lower and lower elevations. Midway along the room length, the jet has entrained air flow at the source height, blowing contaminant in the direction of the jet (i.e., the X direction). As the plume travels in this direction, downwind of the source, turbulent diffusion spreads the plume vertically also. The combined convective and diffusive transport resulted in the concentration patterns shown in Figures 2A and 2B. The highest concentration predicted in the breathing zone was at a horizontal distance of 1.2 m from the source center, not directly above the source, because some travel time was required for the plume to diffuse the 0.5 m from the source level to the breathing zone level.

The concentration pattern shown in Figure 2A also results from a flow of air and contaminant back toward the inlet. Air blown across the source toward the wall farthest from the inlet

(the right wall) was predicted to swirl back, predominantly along the back wall, carrying the contaminant back toward the left wall. This results in higher concentrations near the back and left walls than in areas much closer to the source but upwind. Thus, interpreting the room air flow pattern is essential in determining where the highest contaminant concentrations and worker exposures are likely to occur.

The simulated contaminant concentration contours and velocity vectors for the ceiling diffuser reveal a very different pattern, shown in Figures 2C, 2D, and 3B, also at an air exchange rate of 4 ACH. Here air blows along the ceiling in all horizontal directions, down the walls and back toward the center of the room, along the floor. As the air flow along the floor converges near the table, the flow turns upward and the air speed increases. The contaminant plume moves vertically toward the diffuser, where it becomes entrained in and mixes with the incoming

**TABLE II**

Summary statistics for  $K_m$  within two simulated rooms by air inlet configuration (Dilution air flow rate = 4 ACH)

Statistic	Wall jet	Ceiling diffuser
N	25,600	25,600
Mean	1.13	1.18
Std. deviation	0.42	0.76
Max	19	67
99th percentile	2.1	1.6
1st percentile	0.33	0.98
Min	0.0024	0.0076

dilution air. Thus, the highest breathing zone concentration is almost directly above the source.

Separately for each of the two air inlets studied,  $K_m$  was calculated at each solution node by regression of  $G/Q$  on  $C$ . A straight line through the origin fit these data very well; the lowest  $R^2$  value was 0.97, suggesting that the inverse proportionality of  $C$  to  $Q$  holds very well at each point over the wide range of flow rates studied.  $K_m$  is the slope of the  $C$  versus  $G/Q$  line. Thus, the value of  $K_m$  at a point indicates the sensitivity of concentration to changes in dilution air flow rate. The higher the concentration, the more sensitive concentration is to changes in flow rate for constant  $G$ . In summary,  $K_m$  was constant at each point through the range of flow rates, but varied substantially with location in the room.

Summary statistics of  $K_m$  for the two inlet configurations are shown in Table II. Both room mean  $K_m$  moderately exceeded one, the  $K_m$  of a completely mixed room with the same emission and dilution flow rates ( $K_m = G/Q$ ). Between the 1st and 99th percentiles, the ceiling diffuser simulation yielded a narrower distribution of  $K_m$  values than the wall jet simulation, as a result of a narrower distribution of simulated contaminant concentrations.

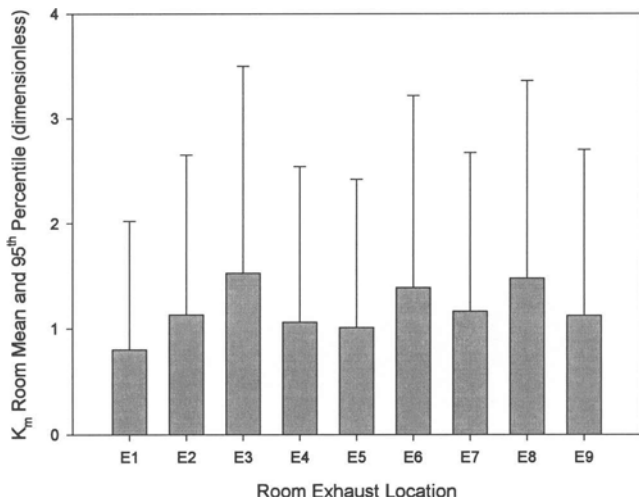
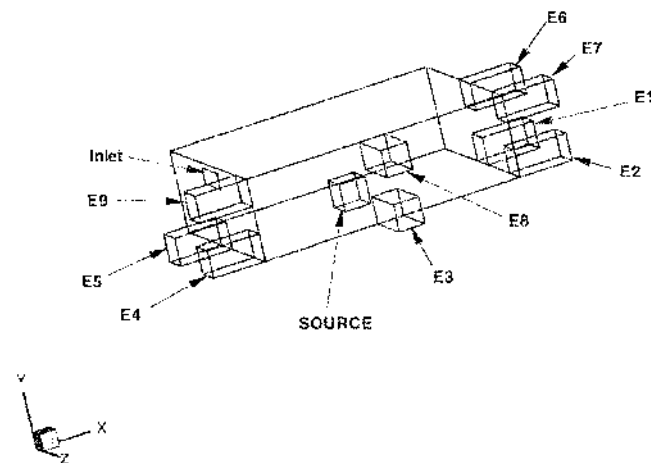


**FIGURE 5**

Mean and 95th percentile of  $K_m$  by exhaust location for wall jet inlet.

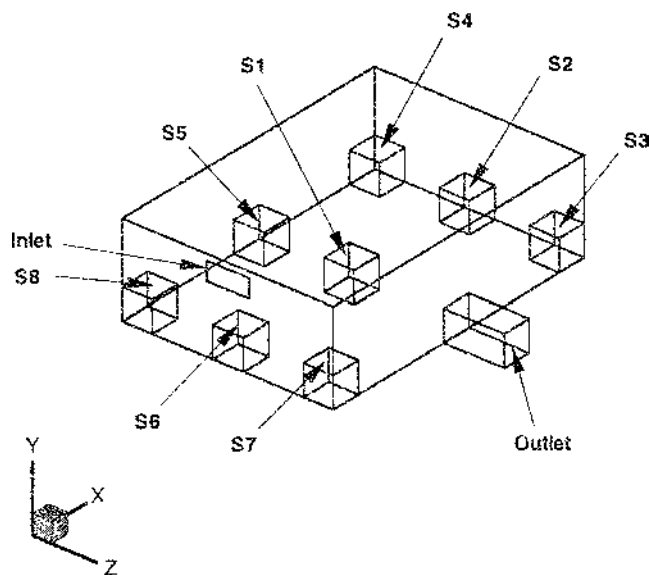
**Simulations of Hypothetical Rooms with Varying Exhaust and Source Locations**

Figure 4 shows the locations of exhaust openings investigated in the simulations and Figure 5 presents the corresponding room  $K_m$  mean and 95th percentile for these configurations. Exhaust locations E3, E6, and E8 gave the highest mean and 95th percentile values. E6 is directly opposite the inlet and produced the greatest degree of short-circuiting of clean dilution air. Location E1 gave the lowest mean and 95th percentile. The mean was about 30 percent less than the  $K_m$  of a completely mixed room for this emission rate and air flow rate. For this location, the inlet



**FIGURE 4**

Exhaust locations studied for the wall jet inlet. (Exhaust locations indicated by "E#").



**FIGURE 6**

Source locations studied for the wall jet inlet. (Source locations indicated by "S#").

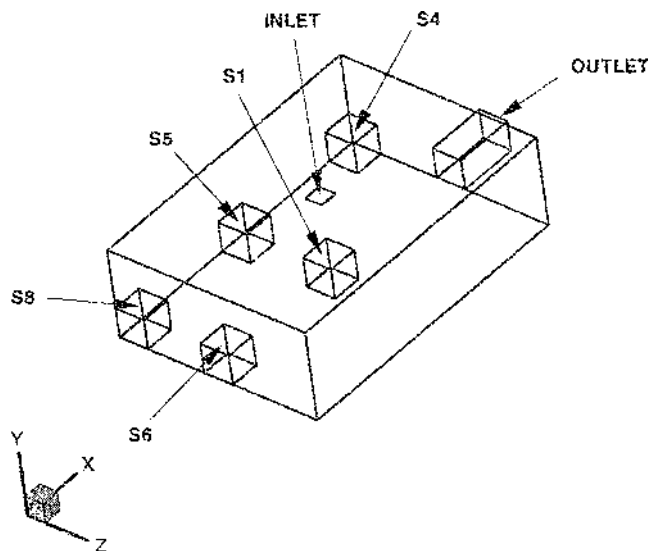


FIGURE 7

Source locations studied for the ceiling diffuser inlet. (Source locations indicated by "S#").

jet expands and carries some of the contaminant directly toward the exhaust.

Figures 6 and 7 show the location of sources studied for the wall jet and ceiling diffuser inlets. Figure 8 presents the corresponding room  $K_m$  statistics for both inlets. For the wall jet, the highest 95th percentile  $K_m$  occurred when the source was positioned against a wall or in a corner. The presence of walls close to the source, in most instances, reduced the dilution near the source. Thus, the 95th percentile  $K_m$  was higher for these source locations. However, one corner location, S3, produced the lowest concentration mean and 95th percentile values of all

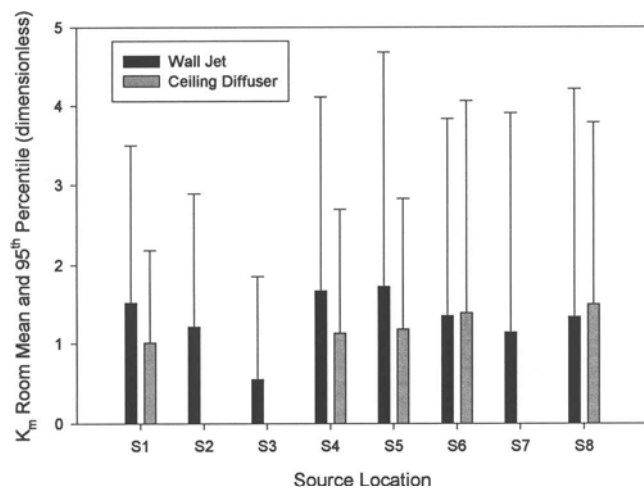


FIGURE 8

Mean and 95th percentile of  $K_m$  by source location for wall jet and ceiling diffuser inlets.

the room configurations studied. In this arrangement, contaminants emanating from the source are carried along the near wall directly to the capture zone of the exhaust opening. Thus, a large fraction of the contaminant plume leaves the room before mixing with room air. The centered source location (S1) gave the lowest  $K_m$  mean and 95th percentiles for the ceiling diffuser, but relatively high  $K_m$  for the wall jet.

For the ceiling diffuser, the highest 95th percentiles occurred for the wall and corner locations farthest from the exhaust opening. The lowest room mean  $K_m$  was observed for the source in the center of the room, similar to the distribution pattern observed in Figure 3. For three source locations, the ceiling diffuser gave lower means and 95th percentiles than the wall jet. For the other two locations simulated for both inlets, the  $K_m$  statistics were nearly the same for both inlet types. Thus, the ceiling diffuser generally produced contaminant concentrations lower than or equal to those observed for the wall jet.

## DISCUSSION

The variation of local  $K_m$  values within a room can be explained partly by the presence of well ventilated and poorly ventilated regions. However, interpretation of the local  $K_m$  values as an indicator of ventilation effectiveness must be approached carefully. High local  $K_m$  at some point does not necessarily indicate that less dilution air is delivered there. Local  $K_m$  equals  $CQ/G$ , where  $Q$  and  $G$  are not functions of position within the room, but apply to the room as a whole. Thus,  $K_m$  is directly related to  $C$ , the local concentration. The local concentration, in turn, is a complex function of the relevant source characteristics (such as location, and emission flow rate, velocity, and density) and all the factors controlling the room air flow pattern. At a fixed point, a higher steady-state concentration and a corresponding higher  $K_m$  mean that less contaminant dilution occurred during transport of contaminant from the source to that point than to points with lower  $C$  and  $K_m$  values.

In a room simulated here, if concentration at a fixed point is to be reduced by dilution to some exposure limit, then the higher the  $C$  and  $K_m$  values are at that point, the higher the design  $Q$  must be. To illustrate how local concentration and the proportionality between  $C$  and  $Q$  determines dilution flow rate requirements, consider two points in one of the rooms simulated here (concentration for complete mixing =  $G/Q = 100$  ppm). Point 1 has a concentration,  $C_1$ , of 150 ppm; point 2 has a concentration,  $C_2$ , of 125 ppm; and, the target exposure limit,  $C_{EL}$ , is 75 ppm. Because concentration is inversely proportional to dilution flow rate in the rooms studied, reduction of  $C_1$  to the  $C_{EL}$  will require a factor of 2 ( $= C_1/C_{EL}$ ) increase in  $Q$ , while reduction of  $C_2$  will require a factor of 1.7 ( $= C_2/C_{EL}$ ) increase in  $Q$ . The  $K_m$  values at points 1 and 2 are 1.5 and 1.25.

The findings of this article suggest several approaches for improving the practice of dilution ventilation for protecting human health. To facilitate their use, the methods for utilizing  $K_m$  are put in a broader context below by discussing them with other ventilation issues and approaches.

### Using Air Monitoring Results

The simulations with varying flow rates indicate that concentration at each point within a room is inversely proportional to flow rate with all other boundary conditions held constant. This finding agrees with earlier work that showed this relationship, but considered fewer room locations, in a simulation of an embalming room.<sup>(12)</sup> Specifying dilution ventilation flow rate for controlling exposure at a specific room location, for instance a workstation, could make use of this finding. Consider a room with inadequate dilution ventilation for which the dilution air flow rate is measurable and air monitoring results exceed an exposure limit ( $C_{EL}$ ), a concentration believed to be safe for the duration and time pattern of an occupant's exposure. A common approach for occupational settings suggests the use of Eq. 1. The emission rate must be determined in some fashion,<sup>(4,5)</sup> for instance by mass balance calculations, emission factors, or simple mathematical models. The value of  $K$  also must be estimated by subjective approaches, that is, "professional judgement." Finally, the  $C_{EL}$  is substituted for  $C$  in Eq. 1, and the required flow rate calculated. The alternative approach suggested by these simulations is to make direct use of the inverse proportionality between  $C$  and  $Q$ , as in Bennett et al.<sup>(12)</sup> The design flow rate,  $Q_d$ , may then be calculated as:

$$Q_d = (K/K_m) \cdot Q_o \cdot (C_o/C_{EL}) \quad [3]$$

where

- $Q_d$  = the design flow rate,
- $Q_o$  = current flow rate,
- $C_o$  = current exposure concentration, and
- $C_{EL}$  = exposure limit.

$K/K_m$  is the safety factor based on all relevant factors except mixing.

This approach avoids the difficulty and uncertainty of estimating  $G$ , and the subjectivity of accounting for incomplete mixing in the safety factor used. The mixing effect is accounted for intrinsically by use of the measured concentration. If the inverse proportionality of  $C$  and  $Q$  can be shown to hold nearly as well in practice as in these simulations, this method represents a much more accurate and objective means of accounting for nonuniform mixing than the traditional approach. In addition, it relies on the data most frequently available in industrial hygiene practice—personal exposure measurements. Finally,  $K/K_m$  may be taken to be one when factors other than mixing, such as uncertainty and effect severity, are built into the  $C_{EL}$ , as is often the case. This may be determined by considering the protocols used to derive the specific  $C_{EL}$ .

This approach also may be extended to situations in which the room occupant does not remain at a fixed location. The path an occupant follows within a room is made up of a set of points. If  $C$  at each of these points is proportional to  $Q$ , then the average  $C$  along the occupant's path also is proportional to  $Q$ . Thus, the approach described above is also applicable to a moving room occupant whose exposure has been well characterized.

### Increasing Room Mixing Versus Limiting Room Mixing

A cursory consideration of these results may suggest increasing mixing to reduce the required  $K_m$  value. Mixing may be increased by proper direction of the incoming air jet or by mechanical agitation, for instance with a ceiling fan or a pedestal fan. However, this is inadvisable if increasing room air movement might interfere with other exposure control methods that rely on keeping incoming clean air and source emissions segregated. These methods include local exhaust ventilation, air islands<sup>(19)</sup>, air curtains or push-pull systems<sup>(1,7)</sup>, and displacement or plug-flow ventilation.<sup>(6,7)</sup> These approaches generally are more effective and reliable than dilution ventilation when interference by extraneous air currents is avoided.

The attractiveness of enhancing mixing increases when:

1. altered flow patterns will not carry contaminants to an occupant's breathing zone before mixing with dilution air;
2. flow patterns can be controlled to sweep contaminants toward exhaust openings;
3. enhanced mixing will not increase contaminant emission rate (for instance, when air flow near the surface of an evaporating liquid increases);
4. other more effective approaches are not feasible; and
5. the objective is to decrease potential exposure throughout the room, not just at a specific occupant location.

Because the effects of room air flow pattern changes may be difficult to predict, subsequent assessment (for instance, by air monitoring) of the effect of increased mixing on exposure is prudent.

When the intent of dilution ventilation is to reduce contaminant concentrations throughout the room, one of the upper percentiles of  $K_m$  could be used as a design parameter in Eq. 1. For the various room configurations studied here, the 95th percentile of  $K_m$  ranged from 1.2 to 3.0, and the 99th percentile ranged from 1.6 to 6.0. If the  $n$ th percentile of  $K_m$  is used in Eq. 1, then about  $(100-n)$  percent of the room volume will exceed the  $C_{EL}$ . The 95th and 99th percentiles in these simulations were at mean distances from the source of 3.5 m (1.4 m Std. Dev.) and 1.9 m (0.9 Std. Dev.), respectively. Based on the CFD results for the room conditions simulated, the 99th percentile of  $K_m$  would protect most occupants further than about 3.7 m (mean + 2 std. dev.) directly downwind of the source, and those much closer in other directions from the source. Under convective air flow, it appears that the 95th percentile of  $K_m$  can be found quite far from the source and may not be appropriate for specifying dilution ventilation flow rates, since exposures downwind of the source would then exceed the  $C_{EL}$ .

Because the required flow rate, and thus cost, increases with increasing  $K_m$ , use of  $K_m$  values in excess of 2 to 3 generally is not economically feasible.<sup>(4)</sup> If mixing considerations suggest higher mixing factors should be used, then other control measures should be considered. In such cases, the pronounced spatial variability may make local ventilation techniques more

efficient than general ventilation and may provide economic motivation for process changes that reduce contaminant emission rate, toxicity, or both.

## CONCLUSIONS AND RECOMMENDATIONS

Limitations of this research include the following:

1. The room configurations studied here follow guidelines for good comfort ventilation regarding room size and location of inlets. Poorly ventilated spaces may require even higher  $K_m$  values, alternative placement of inlets or exhausts, or improved mixing.
2. The effects of natural convection were not investigated. Addition of natural convection likely will increase the degree of mixing and reduce the average  $K_m$ .
3. In simulating the effects of flow rate change, all other boundary conditions were held constant. The constant spatial pattern of  $K_m$  over the flow rate range explored required that the relative velocity profile across the air inlet be kept constant. That is, the velocity at each position on the inlet face varied proportionally to the flow rate.
4. This study explored a source with a constant emission rate, because the concentrations in a room are often directly proportional to the emission rate. However, these findings may not apply to sources with varying emission rates, momentum changes sufficient to alter room air flow patterns, or significant emission density changes.

Based on the validation analyses, it appears that the CFD approaches employed in this study may be used to generate plausible concentration distributions for various room configurations. Simulations of two inlet types each revealed that the mixing factor was constant at fixed points throughout the room over a range of air exchange rates from 1 to 16 air changes per hour, keeping all other boundary conditions constant. Varying exhaust outlet and source locations at constant air flow rate and contaminant emission rate affected the room mean  $K_m$  and the upper  $K_m$  percentiles. The lowest mean concentrations, and thus the lowest mean  $K_m$  values, resulted from convection of emissions directly toward the room exhaust opening. The highest mean concentrations and  $K_m$  values resulted from portions of the incoming dilution air “short circuiting” to the outlet, before mixing with room air.

For the wall jet inlet, sources located against walls and in corners produced the highest 95th percentile  $K_m$  values, with the exception of one source located so that emissions were transported directly to the outlet. For the ceiling diffuser inlet, the highest concentrations resulted from wall and corner sources farthest from the outlet. For this inlet, the source at the room center produced the lowest mean concentration. In general, the ceiling diffuser produced contaminant concentrations and  $K_m$  values lower than or equal to those produced by the wall jet for the same source location. Nevertheless, ceiling diffusers should be employed with caution in industry because their use in such setting is not well studied.

These simulations suggest improvements and limitations for dilution ventilation design. When change to an existing dilution ventilation system is motivated by measured overexposure of room occupants and the existing dilution flow rate can be determined, this study suggests that the ratio of the current exposure concentration to the  $C_{EL}$  (Eq. 3) can provide a more accurate means of accounting for incomplete room mixing than the familiar “K-factor” approach (Eq. 1). Proper application of this method requires that the inlet air velocity at individual points across the inlet face vary proportionally to the flow rate. Thus, elbows close to air inlets should be equipped with turning vanes or system modifications to promote uniform inlet velocity. Also, if an occupant’s exposure varies significantly, the exposure measurements used in Eq. 3 must characterize the full range of exposure.

When the purpose of dilution ventilation is to reduce concentration throughout a room rather than at a specific location, use of the 99th percentile of  $K_m$  as a design parameter to account for mixing may be feasible. However, other control measures should be considered if  $K_m$  exceeds 2 to 3.

$K_m$  may be reduced by enhancing room mixing with fans or altering air inlet configuration. However, mixing should not be increased if the altered room air currents could transport contaminant to an occupant’s breathing zone or interfere with other control methods that depend on segregation of incoming air and contaminant. These other approaches, including local exhaust, air islands, push-pull systems, and displacement flow, frequently are more effective than dilution ventilation when properly designed and maintained.

Finally, it is recommended that standard ventilation design references, such as the American Conference of Governmental Industrial Hygienists (ACGIH<sup>®</sup>) ventilation manual<sup>(1)</sup> and ASHRAE Standard,<sup>(6)</sup> expand their discussion of the effects of mixing, the use of exposure measurements in ventilation design, and comparisons of dilution ventilation with other ventilation strategies.

## ACKNOWLEDGMENT

The authors acknowledge the National Institute for Occupational Safety and Health for support of this research through the cooperative agreement between the Centers for Disease Control and Prevention and the Association of Schools of Public Health, ASPH Project Number S646-17/17.

## GLOSSARY

**Air speed**—Air movement at any location may be characterized by speed or velocity. Speed is simply the distance, in any direction, moved by the air in a unit of time; velocity is a vector quantity including both the speed and the direction of motion. Speed may be expressed as a single number, whereas velocity in three-dimensional flow requires three numbers; for instance, the velocity components in the three directions of an orthogonal coordinate system. At speeds typical of rooms, speed may be

measured with a thermoanemometer, like those used for field industrial hygiene measurements. Velocity determination requires instruments capable of measuring air speed and direction. This is usually done by measuring speed in three separate directions.

**Boundary conditions**—In CFD, the properties of a boundary of the space in which a solution is to be performed. Some boundary conditions in CFD room simulation are wall surface temperature, surface roughness, and inlet gas velocity and composition.

**Cell**—In CFD simulation for fluid motion in three dimensions, the volume (in this case, a room) is divided into a large number of smaller volumes called cells. The CFD program keeps an account of flow properties, such as energy, momentum, or chemical species, in each cell. CFD solutions keep track of the transport of these properties between adjacent cells, and the processes that generate or dissipate these properties within each cell.

**Turbulence length scale**—A physical quantity related to the size of the large eddies that contain the energy in turbulent flows.

**Convergence**—In CFD, the approach to a solution in an iterative (i.e., trial and error) method as indicated by the decrease in the sum of the residuals from one iteration to the next.

**Directionless magnitude of velocity**—See “air speed.”

**Eddy**—A fluid parcel, or a collection of fluid molecules that move with roughly the same speed and rotational direction.

**Grid**—A set of spatial points at which the conservation equations are solved.

**Node**—A point within a grid at which flow properties such as pressure, velocity, momentum, and chemical species are estimated.

**Normalized residual**—A variable’s residual divided by the value of the variable.

**Residual**—In CFD, the difference in a variable’s estimated value from one iteration of the solution to the next.

**Sum of the normalized residuals**—The sum of the normalized residuals over all variables (such as pressure, velocity, and concentration) on a particular iteration of the solution.

**Turbulence intensity**—The root mean square of turbulent velocity fluctuations. Where the instantaneous velocity in a given direction, for example the x direction, is comprised of the average velocity,  $\bar{u}_x$ , and the turbulent fluctuation about the mean,  $u'_x$ , then the turbulence intensity, I, is expressed as:

$$I = \frac{\sqrt{\frac{1}{3} (\overline{u_x'^2} + \overline{u_y'^2} + \overline{u_z'^2})}}{|\bar{u}|}$$

**Turbulence model**—The fundamental conservation relationships for turbulent flow have more unknowns than equations. These equations cannot be solved unless additional equations are employed. The turbulence models provide such additional equations by relating randomly changing turbulent components of fluid properties to time-averaged components, thus enabling solution.

**Turbulent velocity fluctuations**—Air velocity is considered to consist of a steady-state (i.e., time averaged) component and a

rapidly fluctuating, instantaneous component. See “turbulence intensity” above.

## REFERENCES

1. ACGIH: Industrial Ventilation—A Manual of Recommended Practice, pp. 2-2, 2-5. American Conference of Governmental Industrial Hygienists, Cincinnati, OH (1997).
2. Lidwell, O.L.; Lovelock, J.E.: Some Methods for Measuring Ventilation. *J Hyg* 44:326–332 (1946).
3. Brief, R.S.: Simple Way to Determine Air Contaminants. *Air Engineering* 2:39–40 (1960).
4. Burton, D.J.: General Methods for the Control of Airborne Hazards. In: *The Occupational Environment—Its Evaluation and Control*, S.R. DiNardi, Ed., pp. 828–847. American Industrial Hygiene Association, Fairfax, VA (1997).
5. Jayjock, M.A.: Modeling Inhalation Exposure. In: *The Occupational Environment—Its Evaluation and Control*, S.R. DiNardi, Ed., pp. 312–327. American Industrial Hygiene Association, Fairfax, VA (1997).
6. ASHRAE: Ventilation for Acceptable Indoor Air Quality. Standard 62-1999. American Society of Heating, Refrigerating and Air-Conditioning Engineers, Atlanta, GA (1999).
7. Heinsohn, R.J.: *Industrial Ventilation: Engineering Principles*. John Wiley and Sons, New York (1991).
8. Burgess, W.A.; Ellenbecker, M.J.; Treitman, R.D.: *Ventilation for Control of the Work Environment*, p. 98. John Wiley and Sons, New York (1989).
9. Mage, D.T.; Ott, W.R.: The Correction for Nonuniform Mixing in Indoor Microenvironments, EPA/600/A-94/196. Environmental Protection Agency, Research Triangle Park, NC (1994).
10. Patankar, S.V.: *Numerical Heat Transfer and Fluid Flow*. Hemisphere, New York (1980).
11. Emmerick, S.J.: Use of Computational Fluid Dynamics to Analyze Indoor Air Quality Issues, NISTIR 5997. National Institute for Standards and Technology, Gaithersburg, MD (1997).
12. Bennett, J.S.; Feigley, C.E.; Khan, J.; et al.: Comparison of Mathematical Models for Exposure Assessment with Computational Fluid Dynamic Simulation. *Appl Occup Environ Hyg* 15(1):131–144 (2000).
13. Hosni, M.H.; Tsai, K.; Hawkins, A.N.: Numerical Predictions of Room Air Motion. ASME Fluids Division Conference Proceedings, 2 (1996).
14. Awbi, H.B.: *Ventilation of Buildings*. E&FN Spon, London (1991).
15. ASHRAE: Thermal Environmental Conditions for Human Occupancy, Standard 55-1981. American Society for Heating, Refrigerating and Air-Conditioning Engineers, Atlanta, GA (1981).
16. ISO: Moderate Thermal Environments—Determination of the PMV and PPD Indices and Specification of the Conditions for Thermal Comfort, ISO 7730. International Standards Organization, Geneva, Switzerland (1984).
17. Cushman, W.A.; Nielsen, W.J.; Pugsley, R.E.: Workplace Design. Chap. 2. In: *Ergonomic Design for People at Work*, E.M. Eggleton, Ed., vol. 1, p. 26. Van Nostrand Reinhold, New York, NY (1983).
18. Hinze, J.O.: Turbulence. In: *Turbulence*, p. 4. McGraw-Hill, New York (1975).
19. Tsuji, K.; Fukuhara, I.: Protection of Breathing Zone by Uniform Velocity Blowing. *Am Indus Hyg Assoc J* 61:568–574 (2000).